Supporting Information

Ito et al. 10.1073/pnas.0900664106

SI Materials and Methods

Mice and Cell Lines. B6 ($H2^b$), B10 ($H2^b$), and B10.D2 ($H2^d$) mice were purchased from Jackson Laboratory. Armenian hamsters were purchased from Cytogen Research and Development. Plat-E, Jurkat cells, C1498 ($H2^b$), MC47 ($H2^d$), and KZH ($H2^k$) were provided by T. Kitamura (University of Tokyo), W. Yokoyama (Washington University, Saint Louis, MO), and N. Shastri (University of California, Berkeley). JLZ-7 (J7) reporter cells were generated by transfecting the reporter construct into human Jurkat cells as described before (1). Nickel-A (an ampho packaging cell line) was generated by transfecting 293T cells with Ampho env and gag-pol with IRES-puro and IRES-blasticidin, respectively. All experiments on mice were approved by Institutional Animal Care and Use Committee of the University of Minnesota, Minneapolis.

Expression Vectors, Constructs, and Retroviral Transduction. Retrovirus expression vectors [pMX, pMXs, pMX(s)-IRES-GFP, and pMX(s)-IRES-puro] were used (kindly provided by T. Kitamura) (2); pMXs-IRES-human CD4 were generated by inserting the human CD4 cDNA lacking the cytoplasmic domain amplified by PCR; pMX-IRES-Blasticidin was generated similarly. Constructs of Ly49A-CD3ζ chimeric receptor (Ly49AZ) and cytoplasmic deleted Ly49A ($Ly49A^{cyto\text{-}del}$) were generated by PCR as described before (3). Expression plasmids were transfected into Plat-E or Nick-A with FuGENE 6 (Roche) according to manufacturer's instruction. Transduced cells were selected with the same dose of puromycin for each cell type. The lentivirus vector, pEF-SIN (provided by L. Cheng, Johns Hopkins University, Baltimore) (4), was used for lentivirus production. The cDNA for Thy1.1 was a kind gift from S. Jameson, University of Minnesota. The cDNAs for VSVG envelope and the delta-8.9 plasmid (provided by D. Baltimore, California Institute of Technology) (5) were cotransfected with the lentivirus vector into 293T cells. Clonal C1498 cells expressing $H2D^d$ (C1498-Dd) were generated by transduction of the pMXs-$H2D^d$-IRES-hCD4 and by limited dilution after hCD4 enrichment with MACS beads according to the manufacture's instruction (Miltenyi Biotec). GFP-fused Ly49A receptors were constructed and transduced into J7 cells by using pMXs-IRES-puro vector followed by puromycin selection. Clonal C1498 cells expressing RFP-fused $H2D^d$ (D^d-RFP) were generated by transducing pMX-D^d-RFP-IRES-puro into C1498 cells and by limiting dilution (The RFP cDNA was a kind gift from R. Tsien, University of California, San Diego).

Flow Cytometry. Anti-human CD8, anti-$H2K^b$, and anti-Ly49A mAb were purified from the OKT8, AF6–88.5, and A1 hybridoma, respectively. Purified A1 mAbs were conjugated with FITC according to standard methods in our laboratory. The following mAbs were purchased from BD PharMingen or eBioscience: biotin-Ly49A (A1), phycoerythrin (PE), or allophycocyanin (APC)-NK1.1 (PK136), APC-DX5, peridinin chlorophyll-alpha protein–cyanin 5.5 (PerCP-Cy5.5)-CD3 (2C11), biotin-$H2D^d$ (34-2-12), biotin-H-$2K^b$ (AF6-88.5), and PE-IFNγ (XMG1.2). For primary cells, 2.4G2 hybridoma supernatant was used to block FcγRII/III receptors. Flow cytometry was performed on FACSCalibur (BD Biosciences). FlowJo (Tree Star) software was used for analysis.

Cytotoxicity Assay. Lymphokine activated killer (LAK) cells were prepared from mouse spleen as described before (6), with minor modification. Instead of recombinant IL-2, 10% of condition medium from cells expressing IL-2 (kindly provided by M. Colonna, Washington University) was used. On day 5, adherent LAK cells were separated with biotinylated mAb A1 and MACS beads. The proportion of Ly49A-positive cells was >90% in Ly49A-positive LAK cell cultures and <5% in Ly49A-negative LAK cell cultures. Alternatively, GFP^+ and GFP^- or $Thy1.1^+$ and $Thy1.1^-$ LAK cells were sorted on days 4–6 by FACSDiVa (BD Biosciences). More than 95% of cells were NK1.1+ and CD3− unless mentioned. Sorted cells were tested directly on days 8–9 in standard ^{51}Cr-release assays using 96-well round-bottom plates. Ly49A-depleted LAK cells were generated from mice treated with 200 μg of A1 mAb 3 days before the LAK cell preparation. Because A1 mAb completely restores the inhibitory effect by Ly49A engagement of C1498-D^d target cells, the relative inhibitory ability of the mutant receptor is calculated as follows: [(% killing of IRES-Thy1.1 LAK cells) − (% killing of mutant receptor-IRES-Thy1.1 LAK cells)]/[(% killing of IRES-Thy1.1 LAK cells) − (% killing of Ly49A receptor-IRES-Thy1.1 LAK cells)] × 100.

Retrovirus and Lentivirus Transduction into Primary Mouse Cells. Bead-selected CD4 T cells were stimulated with 5 μg/mL ConA and 100 U/mL rhIL-2 in Click's medium containing 10% FCS for 2 days. Viral supernatants were used to infect these CD4 T cells as described before (3). FACS analyses were performed 48 h after the infection. The viral supernatants were used to infect BM hematopoietic precursors as described before (7) with minor changes. Instead of recombinant IL-3 and IL-6, condition medium from X63Ag8 cells expressing IL-3 and IL-6, respectively (kindly provided by H. Karasuyama, Tokyo Medical and Dental University, Tokyo) was used. Infected BM cells were injected into the tail or ocular vein of 9.5-Gy-irradiated B6 mice. Splenocytes were harvested for LAK cell preparation 5–8 weeks after the transplant. The supernatant containing lentivirus was used for infecting day 3 LAK cells using the spin-infection method for 1 h at 2,000 × g in the presence of polybrene (8).

Tetramer Production. The $H2D^d$ tetramers with a motif peptide (9) and the human or mouse β2-microglobulin ($H2D^d$/mβ2m or $H2D^d$/hβ2m) were made according to previously described methods (10). Ly49A tetramers were made according to previously described methods (11) with minor modification. The refolded sLy49A was purified by anion-exchange column chromatography on a monoS with Mes buffer instead of a UNO Q-6 column.

Cytokine Assays. Ninety-six-well plates were coated with anti-Ly49A mAb or isotype control mAb (AF6–88.5) (50 μg/mL in 100 μL) in the presence of anti-NK1.1 mAb (2 μg/mL in 100 μL). LAK cells (2×10^5) were stimulated for 60 min, and then further incubated in the presence of brefeldin A for an additional 4–5 h.

Production of Polyclonal Abs to Ly49A. Armenian hamsters were immunized four times with bacterially prepared and purified His-tagged Ly49A NKD domain. Ten days after the final immunization, the serum was harvested from euthanized hamsters.

Immunoprecipitation and Western Blotting. Clonal C1498 cells expressing Flag-tagged $H2D^d$ (fD^d) was established by the transduction of pMX-fD^d-IRES-Blasticidin with the drug selection and limiting dilution. C1498-fD^d cells were further trans-

duced with Ly49A or ST2 using the pIP vector after puromycin selection. Cells (6×10^6) were washed by PBS and lysed on ice for 4 h in Tris buffer (20 mM Tris, pH 8.0) containing 0.3% Triton X-100, and were immunoprecipitated overnight with anti-flag M2-agarose (Sigma). After 3 washes with lysis buffer, immunoprecipitates were separated by SDS/PAGE (10% gel, reducing condition), transferred onto nitrocellulose membrane, and incubated with hamster anti-Ly49A polyclonal Abs and HRP-conjugated anti-hamster IgG (Jackson ImmunoResearch Laboratories). For detection, an enhanced chemiluminescence kit was used according to the supplier's instructions (Pierce).

Confocal Microscopy. GFP-expressing J7 and C1498-D^d/RFP cells were cocultured at a 1:1 ratio (5×10^4 cells each) in glass-bottom 96-well plate, spun down, and incubated for the indicated time at 37 °C. GFP-expressing LAK and C1498-D^d-RFP cells were cocultured at a 1:2 ratio (5×10^4 vs. 1×10^5 cells each). After incubation, plates were placed on ice and each image was acquired by Olympus FluoView FV1000 inverted microscope (Olympus) using Plan Apo N oil x60/1.42 objective at 1,024 × 1,024 dimension. Sequential acquisition of the GFP-Ly49A (green detector, 500–530 nm) and D^d-RFP signal (red detector, 555–655 nm) was done to avoid cross-talk between GFP and RFP. For immunological synapse (IS) formation with J7 cells, 4 to 5 images of each receptor mutant were acquired in 1 experiment, and experiments were repeated 3 times for each time point. For IS formation with LAK cells, the number of IS per 100 GFP^+ LAK cells was obtained from 7 independent images from 1 well and averaged from 4 independent analyses of a single well. Cell and synapse numbers were counted manually by using the Image J software (National Institutes of Health; http://rsb.info.nih.gov/ij/). The synapse was defined with 3 criteria: (*i*) GFP-expressing cells had a visual cell contact with C1498-D^d/RFP; (*ii*) merged image had yellow color in the cell–cell contacting area; and (*iii*) the contacting region had >2 times integrated fluorescence intensity of GFP at the contacting interface of cells against that at noncontacted membrane region of same J7 cell.

Statistics. Multiple comparisons within each experiment were conducted. The experiment-wise error rate was held to the $\alpha = 0.05$ level by performing a Sidak t test, which held the comparison-wise (or Type I) error rate to $1 - (1 - \alpha)^{1/n}$, where n is the number of comparisons.

1. Sanderson S, Shastri N (1994) LacZ inducible, antigen/MHC-specific T cell hybrids. *Int Immunol* 6:369–376.
2. Kitamura T, et al. (2003) Retrovirus-mediated gene transfer and expression cloning: Powerful tools in functional genomics. *Exp Hematol* 31:1007–1014.
3. Iizuka K, et al. (2007) Protection from lethal infection by adoptive transfer of CD8 T cells genetically engineered to express virus-specific innate immune receptor. *J Immunol* 179:1122–1128.
4. Cui Y, et al. (2002) Targeting transgene expression to antigen-presenting cells derived from lentivirus-transduced engrafting human hematopoietic stem/progenitor cells. *Blood* 99:399–408.
5. Lois C, Hong EJ, Pease S, Brown EJ, Baltimore D (2002) Germline transmission and tissue-specific expression of transgenes delivered by lentiviral vectors. *Science* 295:868–872.
6. Karlhofer FM, Ribaudo RK, Yokoyama WM (1992) MHC class I alloantigen specificity of Ly-49+ IL-2-activated natural killer cells. *Nature* 358:66–70.
7. Furukawa H, Iizuka K, Poursine-Laurent J, Shastri N, Yokoyama WM (2002) A ligand for the murine NK activation receptor Ly-49D: Activation of tolerized NK cells from beta(2)-microglobulin-deficient mice. *J Immunol* 169:126–136.
8. Tran J, Kung SK (2007) Lentiviral vectors mediate stable and efficient gene delivery into primary murine natural killer cells. *Mol Ther* 15:1331–1339.
9. Corr M, Boyd LF, Padlan EA, Margulies DH (1993) H-$2D^d$ exploits a four residue peptide binding motif. *J Exp Med* 178:1877–1892.
10. Altman JD, et al. (1996) Phenotypic analysis of antigen-specific T lymphocytes. *Science* 274:94–96, and erratum (1998) 280:1821.
11. Matsumoto N, Tajima K, Mitsuki M, Yamamoto K (2001) H-2 allele specificity of the NK cell C-type lectin-like MHC class I receptor Ly49A visualized by soluble Ly49A tetramer. *Int Immunol* 13:615–623.

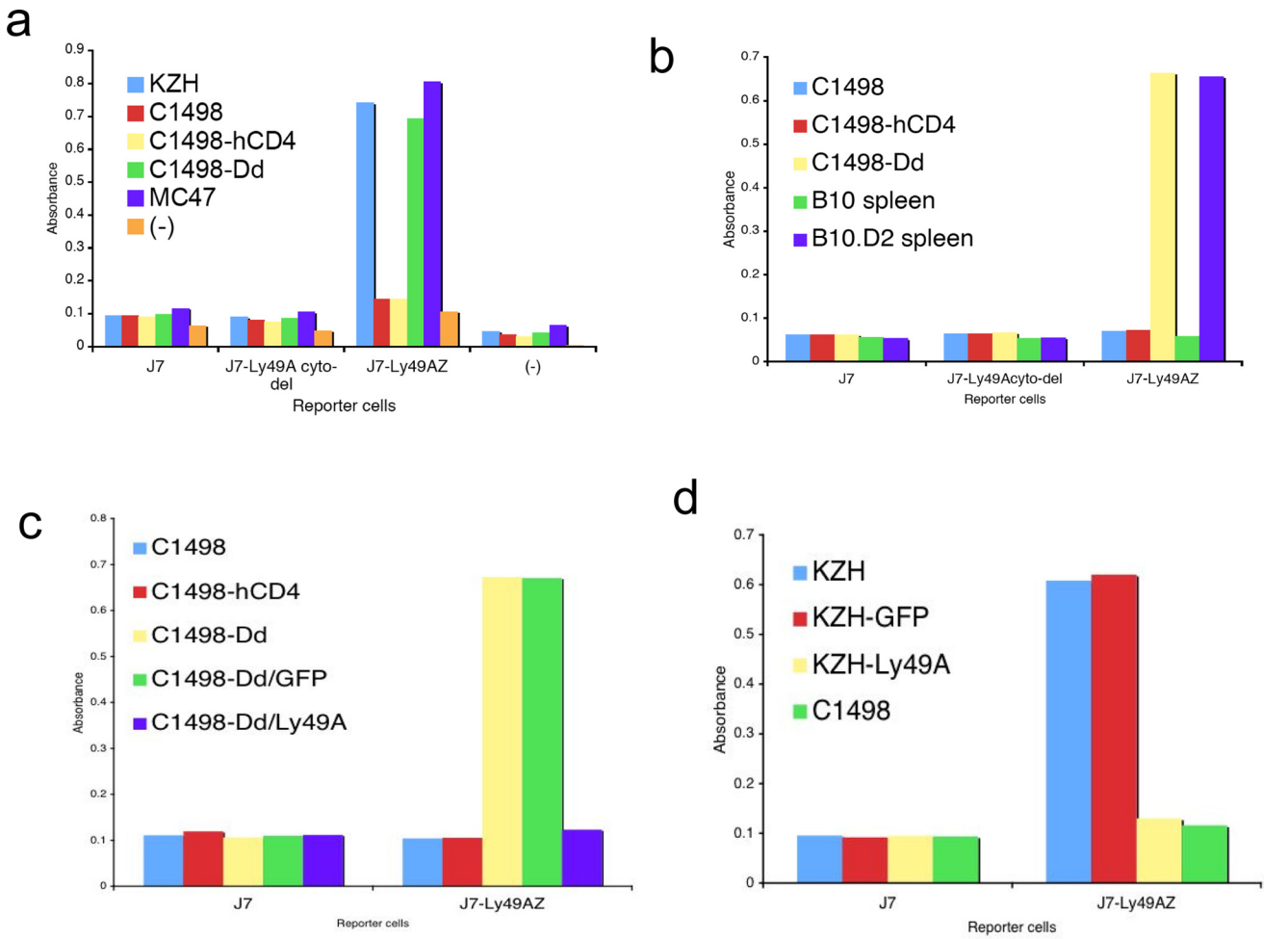

Fig. S1. Establishment of reporter cell assays to detect *cis* and *trans* binding conformations of Ly49A and ligand. (*a*) *Trans* recognition of ligands by Ly49A reporter cells. Indicated target and reporter cells were incubated overnight and subjected to CPRG assays. Each cell line has the following H2 haplotype: KZH ($H2^k$), C1498 ($H2^b$), and MC47 ($H2^d$). C1498-hCD4 was transduced with pMX-IRES-hCD4, serving as control for C1498-D^d. J7-Ly49A cyto-del: J7 cells transduced with the Ly49A lacking the cytoplasmic domain. (*b*) Ly49A reporter assays with primary splenocytes. One-hundred-thousand target cells for C1498 cells and for primary splenocytes from B10 and B10.D2 were cocultured with indicated reporter cells overnight and subjected to CPRG assays. (*c* and *d*) Blockade of *trans* recognitions by ligand receptor *cis* interaction. Reporter cell assays were performed with indicated reporter and target cells.

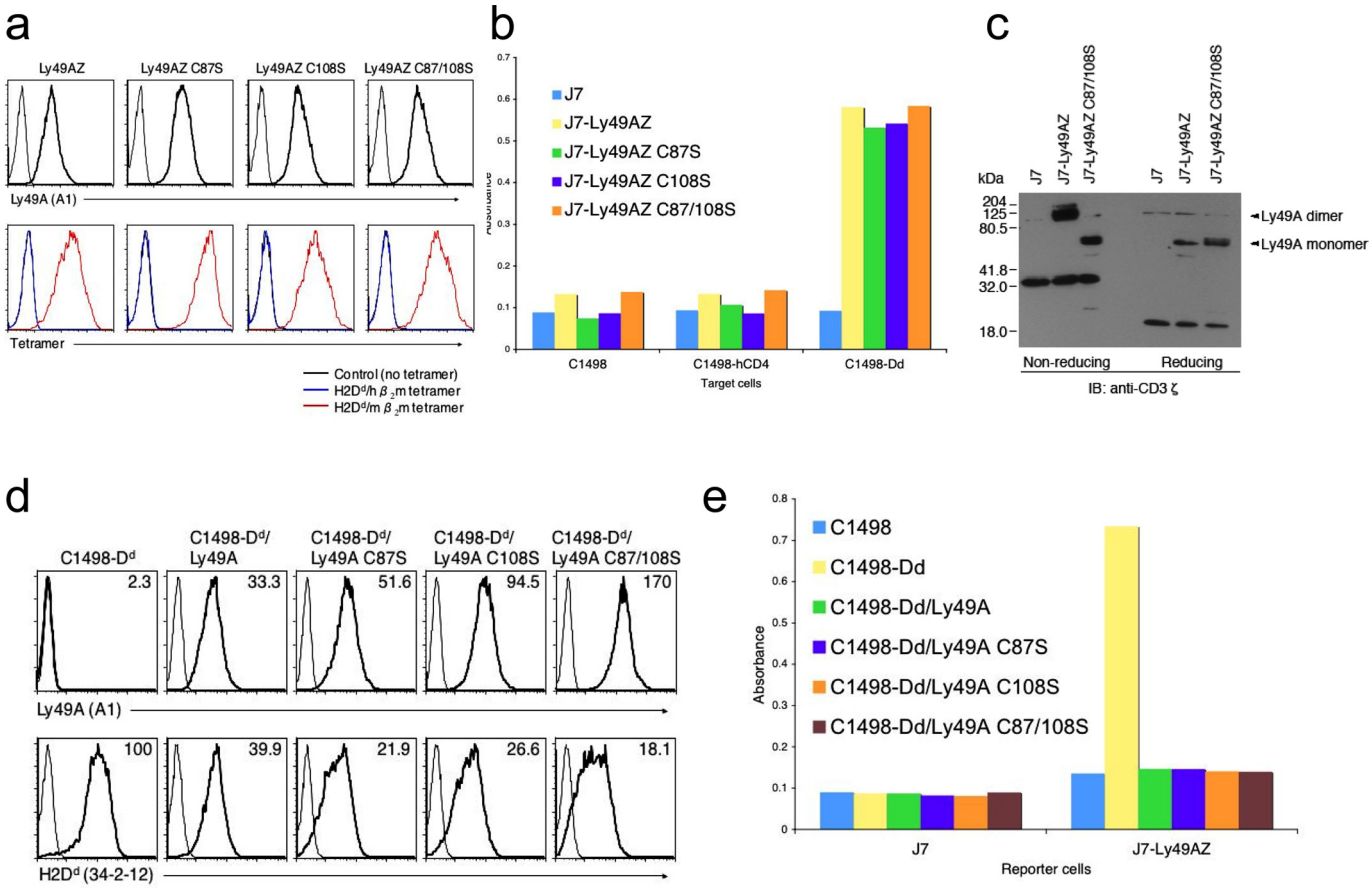

Fig. S2. Cysteines in the Ly49A stalk region are dispensable for ligand in *cis* and *trans* manners. (*a*) Surface expression of the reporter cells expressing the site-directed mutations at cysteines to serines in the Ly49A stalk region. Anti-Ly49A mAb staining and H2D^d tetramer bindings to each reporter cells are shown. (*b*) Reporter cell assays with indicated target cells and reporter cells expressing cysteine mutant Ly49As. Indicated target and reporter cells were incubated overnight and subjected to CPRG assays. (*c*) The total lysates of indicated reporter cells were immunoblotted by anti-CD3ζ mAb under reducing and nonreducing conditions. (*d*) Surface expression of the target cells expressing H2D^d and the site-directed Ly49A mutations at cysteines in the Ly49A stalk region. Anti-Ly49A (A1) mAb staining of each target cells is shown. The MFI value is indicated. Expression levels of the second cistron of the IRES vector, hCD4, were not changed in these double transductants.(*e*) Reporter cell assays with indicated C1498-D^d target cells coexpressing cysteine mutant Ly49As and Ly49A reporter cells.

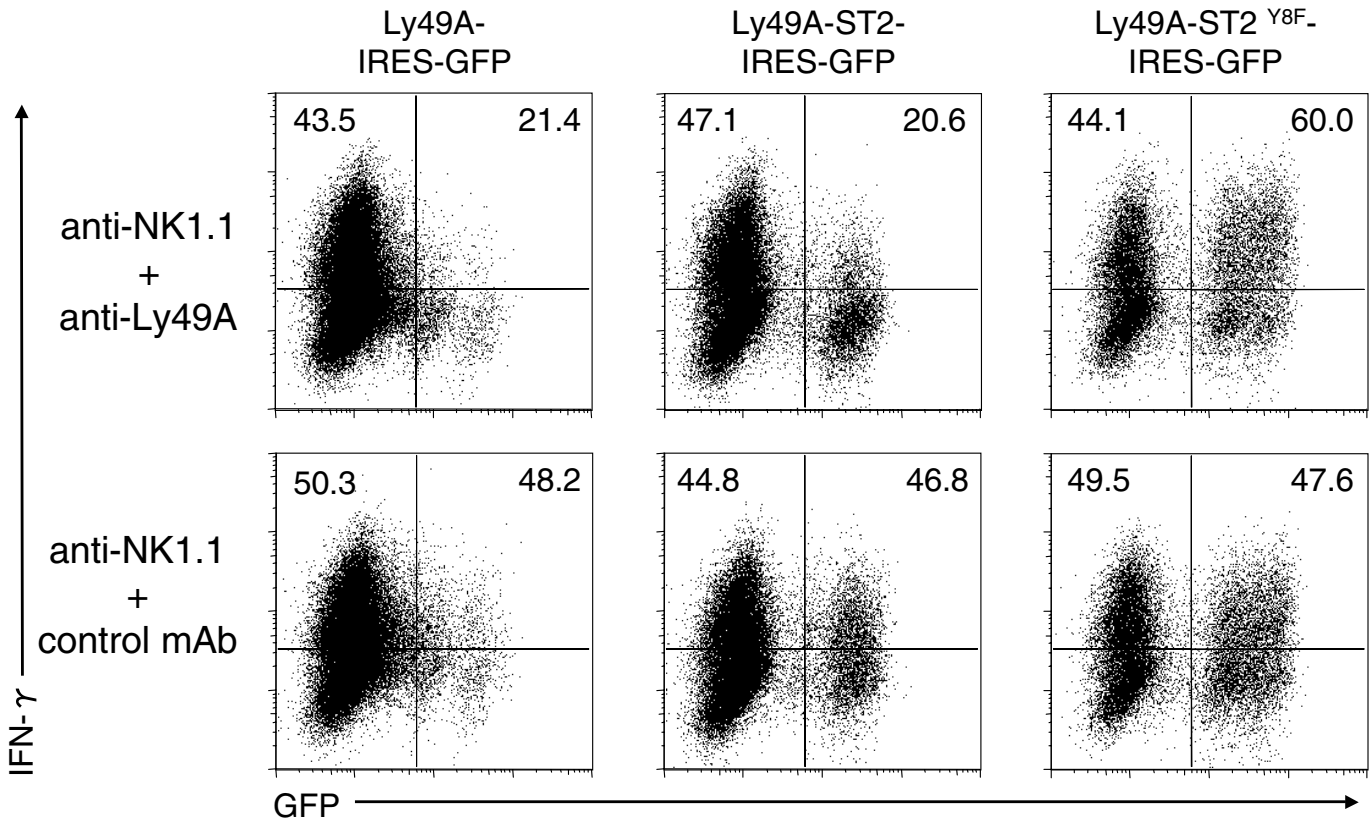

Fig. S3. Signaling ability of Ly49A-ST2 in LAK cells by mAb crosslinking. A Ly49A-ST2 mutant, Ly49A-ST2^{Y8F}, has a Tyr-to-Phe change in the ITIM. LAK cells were generated from BM chimera mediated by retrovirus gene transfer method. LAK cells were cross-linked with the anti-NK1.1 and anti-Ly49A mAb or the anti-NK1.1 and isotype control mAb. Cells were then stained for intracellular IFN-γ. Gated NK1.1^{+}/CD3^{-} cells are shown. Numbers represent the percentages of IFN-γ cells among the GFP^{+} or GFP^{-} cell populations. Representative data from 3 independent experiments are shown.

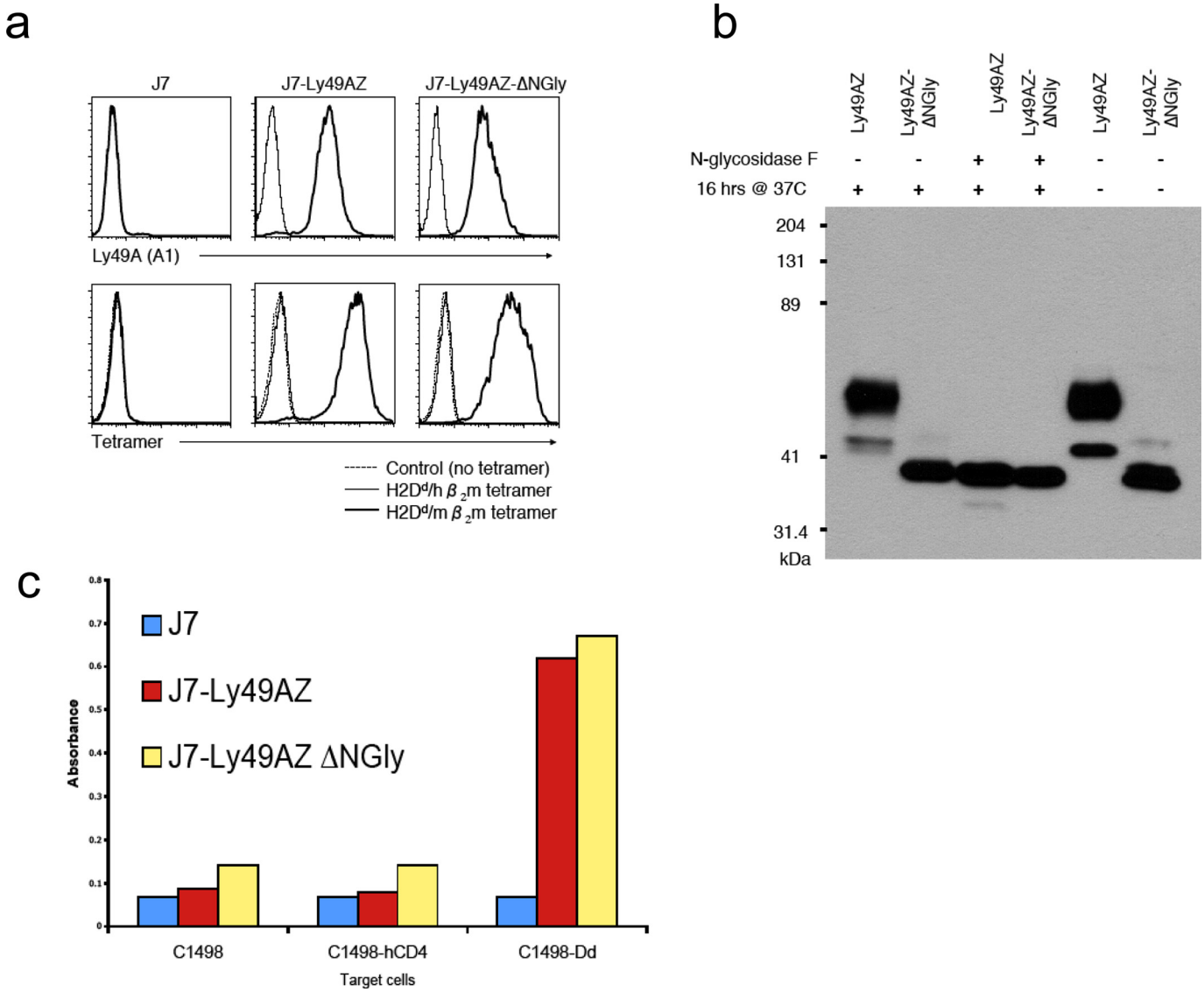

Fig. S4. N-Glycosylations of Ly49A are not involved in the receptor-ligand *trans*-interaction. (*a*) Ly49A surface expression and H2D^d tetramer bindings in J7 reporter cells expressing wild-type Ly49AZ and the N-glycosylation mutant of Ly49AZ (Ly49AZ-ΔNGly). Potential N-glycosylation sites in the stalk region were mutated from asparagines to aspartates and transduced into J7 reporter cells. FACS profiles after puromycin selection are shown. (*b*) The lysate of J7-Ly49AZ or J7-Ly49AZ-dNGly reporter cells was treated with or without N-glycosidase F at 37 °C for 16 h. Samples were applied to SDS/PAGE under reducing conditions and blotted with anti-Ly49A polyclonal Abs. Treatment of Ly49AZ-ΔNGly with N-glycosidase had no effect on its migration, confirming that there are no other N-glycosylation sites on Ly49A. (*c*) Reporter assays performed with H2D^d-expressing target cells and J7-Ly49AZ or J7-Ly49AZ-ΔNGly reporter cells.

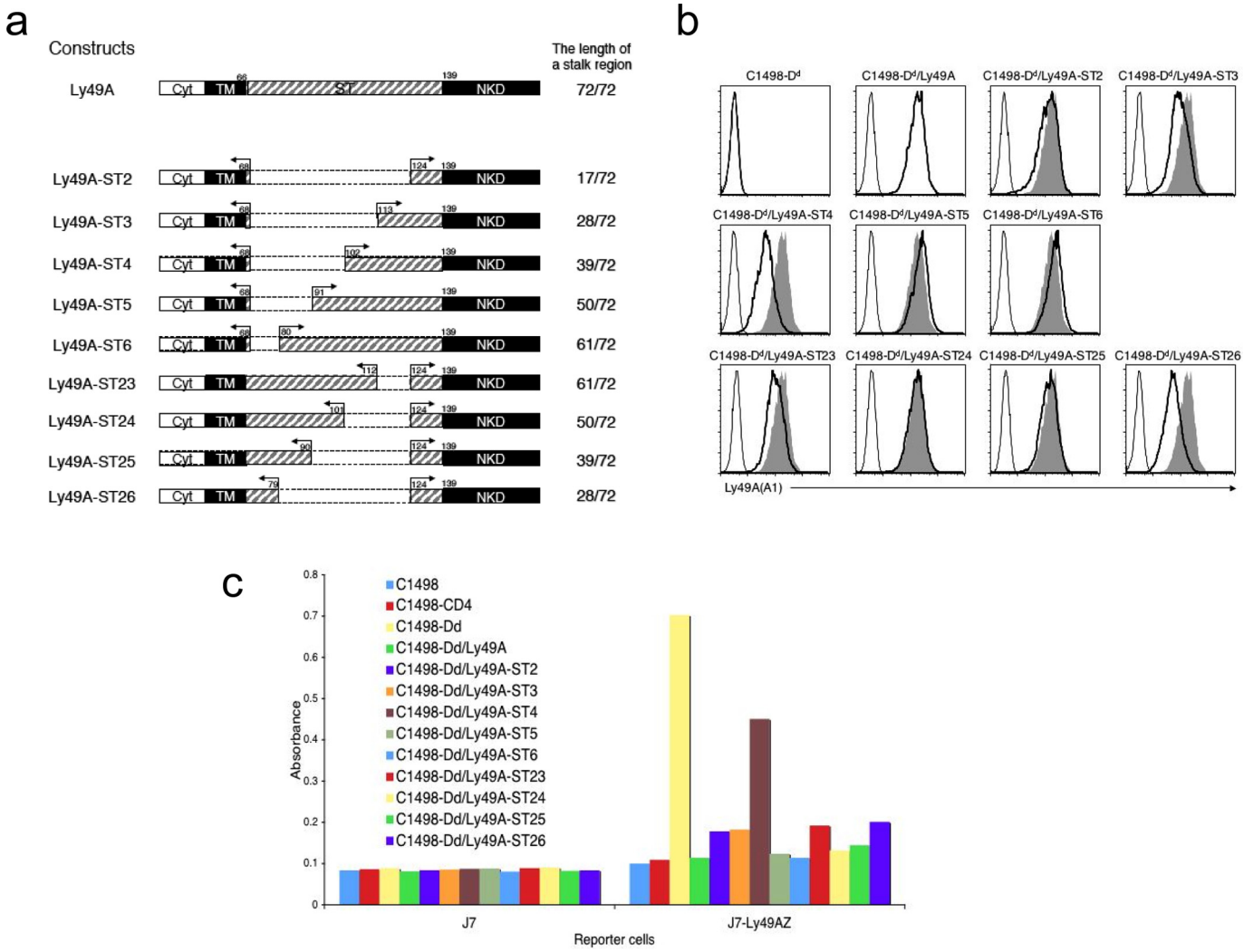

Fig. S5. Requirement of the stalk region for ligand binding in a *trans*, but not in a *cis* manner. (*a*) Schematic representation of stalk-deletion mutant receptors. (*b*) Surface expression of the target cells expressing $H2D^d$ and the stalk deletion mutant Ly49A receptors. A series of stalk deletion Ly49As were transduced by pMXs-IRES-puro vector and selected by the same amount of puromycin. Anti-Ly49A mAb staining to each target cells are shown. Gray shades represent the overlaid histogram of GFP expression from Ly49A. (*c*) Reporter cell assays with Ly49A reporter cells and indicated target cells. (*d*) Expression level of stalk-deletion mutants of Ly49A. All of the stalk-deletion mutant receptors (including Ly49A-ST2 in this figure) were transduced with pMXs-IRES-puro vectors and selected by the same dose of puromycin. Shades represent the overlaid histogram of the anti-Ly49A mAb reactive with J7-Ly49AZ. (e) $H2D^d$ tetramer binding to J7 cells expressing the stalk-deletion mutant receptor. Indicated reporter cells were stained with SA-PE-conjugated $H2D^d/m\beta2m$ or $H2D^d/h\beta2m$ tetramers. Shades represent the overlaid histogram of the $H2D^d/m\beta2m$ tetramer binding to J7-Ly49AZ. (*f*) *Trans* interaction assays with reporter cells expressing the stalk-deletion mutant receptors. Indicated target and reporter cells were incubated overnight and subjected to CPRG assays.

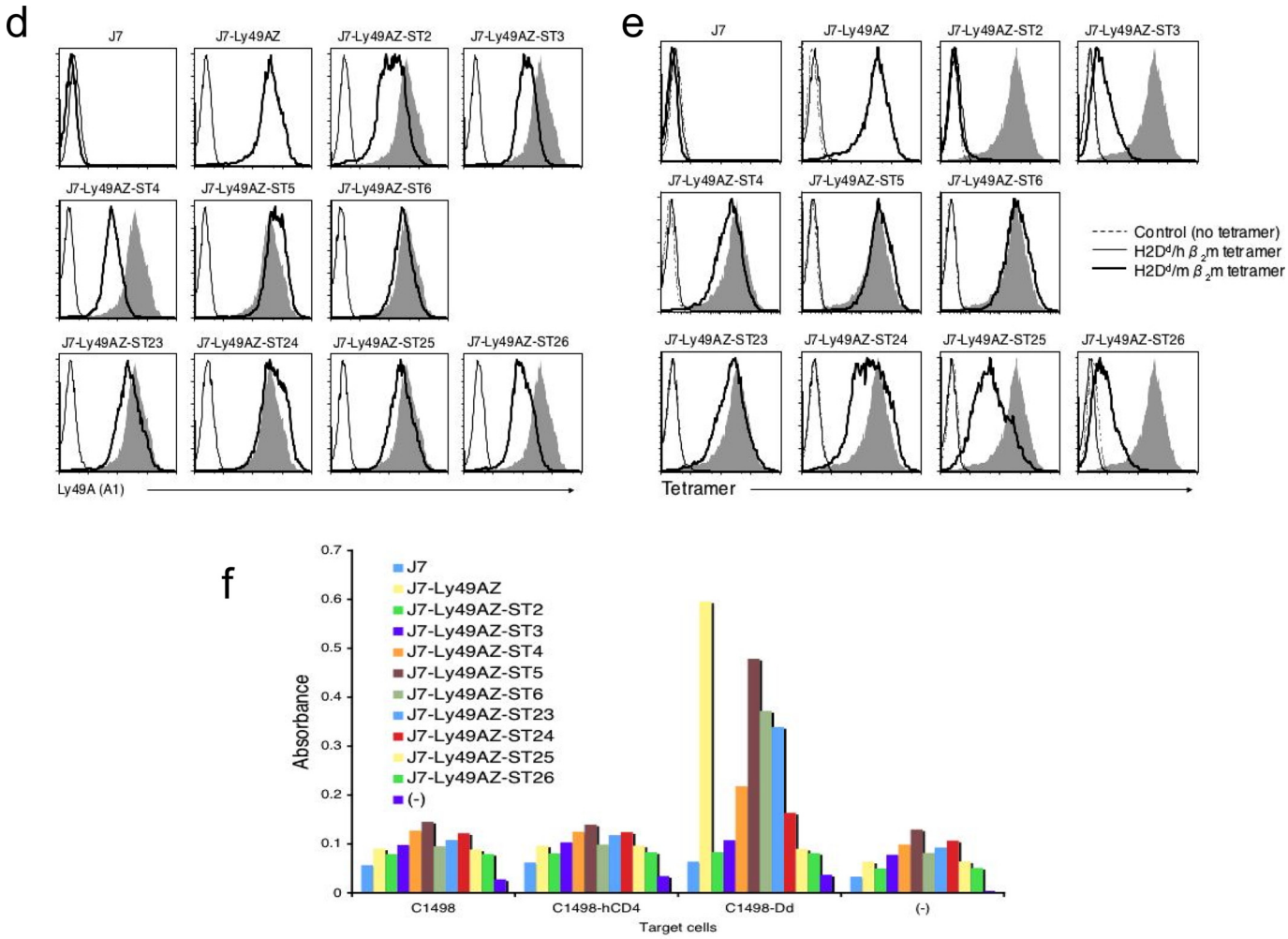

Fig. S5 continued.

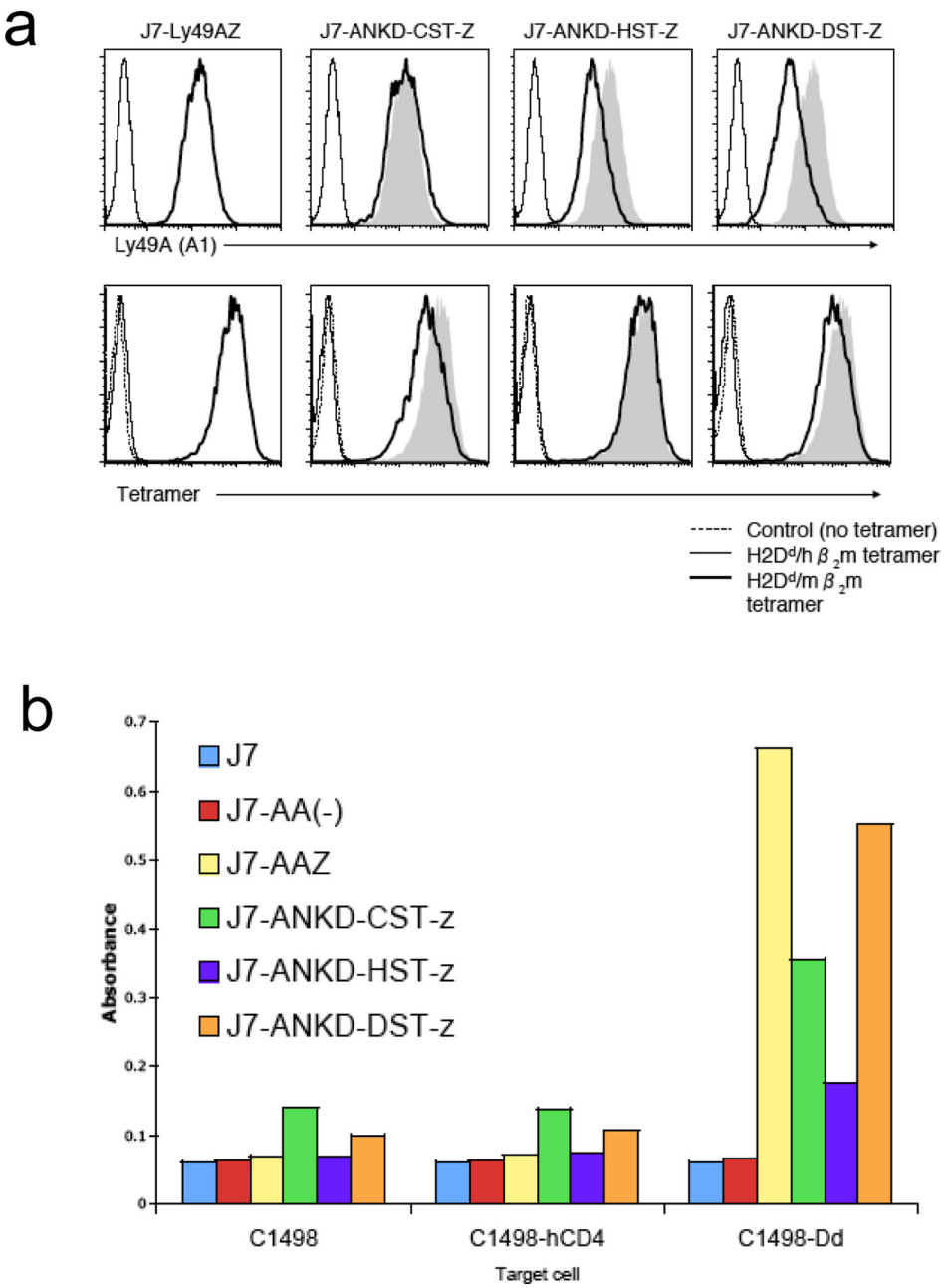

Fig. S6. The stalk-chimeric receptor with the stalk region of Ly49D signals similar to Ly49AZ. (*a*) Surface expression of stalk-chimeric receptors. Ly49AZ, ANKD-CST-Z, ANKD-HST-Z, and ANKD-DST-Z on J7 reporter cells were stained with anti-Ly49A mAb (A1) and H2D^d/mβ2m tetramers. Gray shades represent the overlaid histogram from Ly49AZ. (*b*) Differential signaling ability of stalk-chimeric receptors with stalk regions from the activating Ly49s, Ly49D, and Ly49H. *Trans* interaction reporter assays were performed with indicated target and reporter cells.

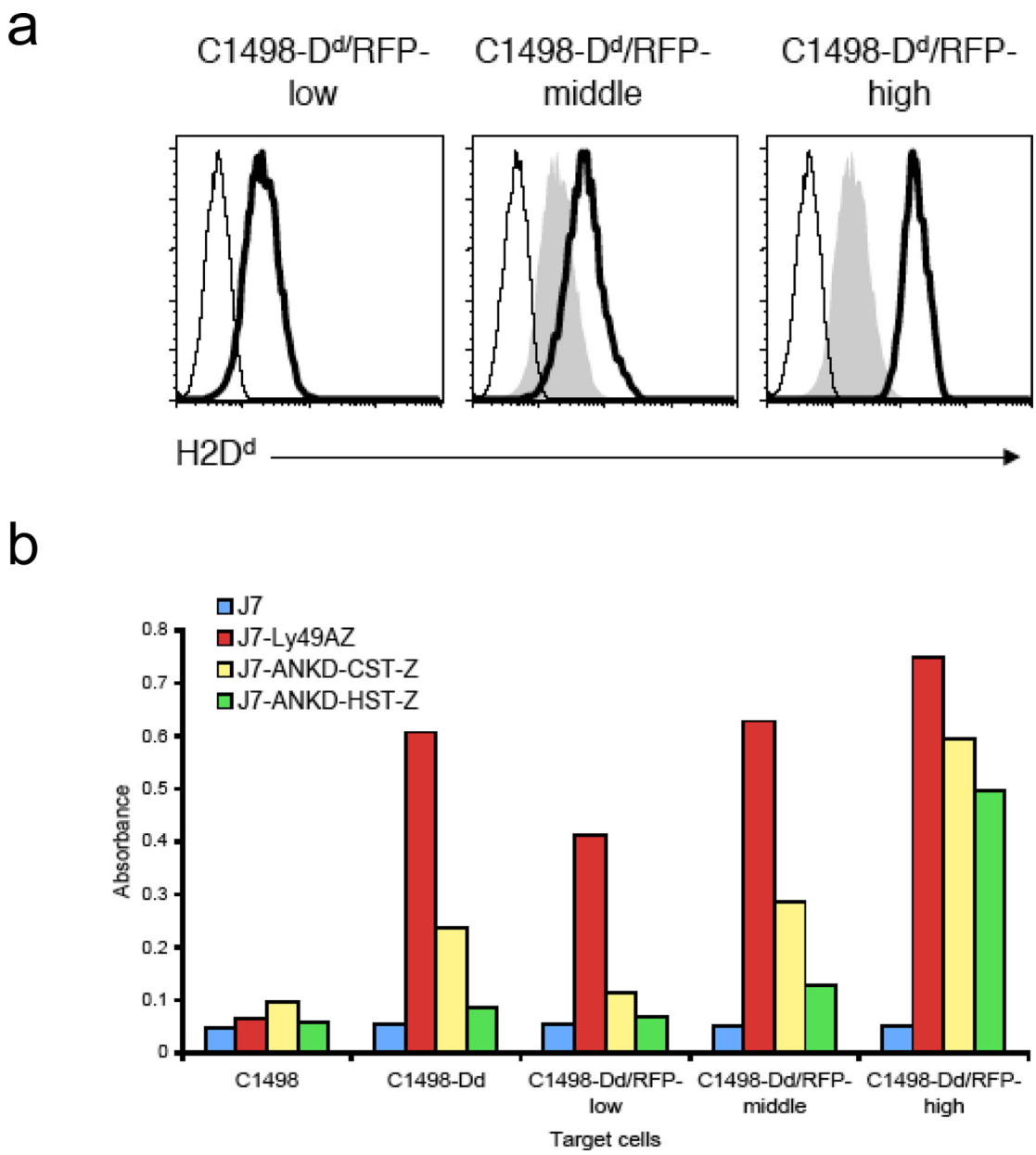

Fig. S7. High avidity condition compensates for the lower signaling ability of stalk-chimeric receptors. (*a*) Expression level of $H2D^d$ on C1498-D^d/RFP target cells. Biotynylated anti-D^d mAb following SA-FITC staining is shown. Gray shades represent the overlaid histogram from C1498-D^d-low. C1498-D^d-high was used in IS formation assays. The expression level of $H2D^d$ of C1498-D^d cells was more similar to C1498-D^d-low and C1498-D^d-mid than to C1498-D^d-high when analyzed in 2 color FACS analysis with compensation. (*b*) *Trans* reporter cell assays were performed with indicated target and effector cells for overnight coculture. In 2-h coculture, a significant difference was not observed among reporter cells. C1498-D^d cells used for the killing, and reporter assays were also used as a reference response.

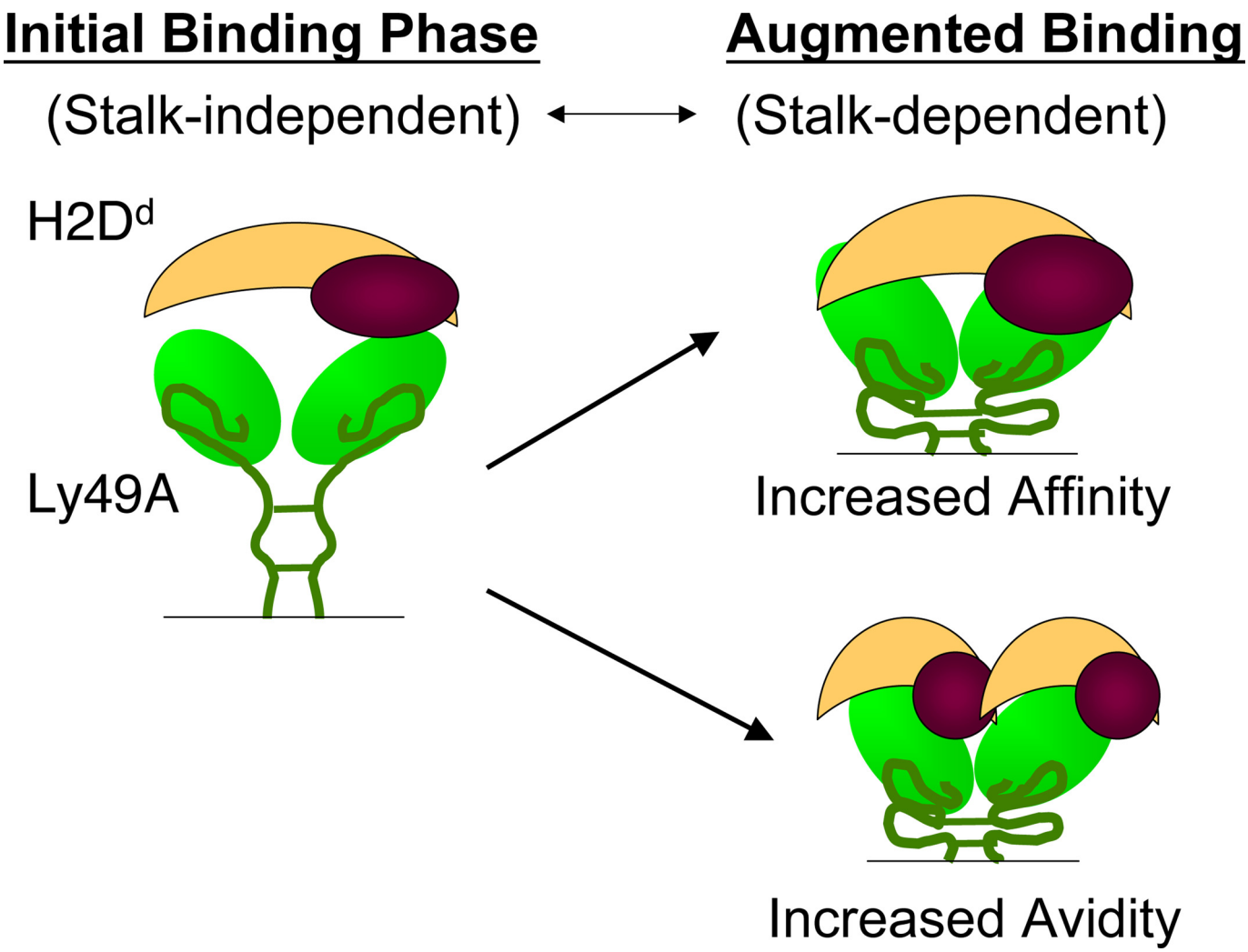

Fig. S8. Proposed model for how the stalk region mediates augmented Ly49A and D^d ligand binding. The initial receptor ligand-binding phase is independent of the stalk region and mainly determined by the molecular structure of receptor-ligand interfaces. The augmented binding phase is achieved by specific interactions between NKD and the stalk region (conformational change of the stalk region), which in turn increases receptor affinity by lowering the off-rate of binding or increases receptor avidity by transforming NKD from a closed to an open conformation that is capable of interacting with 2 ligands. These conformational changes may induce a compaction of the receptor ligand complex, shortening the distance between the target and effector cells, and facilitating surrounding receptors to interact with ligands; thus, forming an IS.

Table S1. Results from experiments with 2-h incubation

	C1498 cells	J7 cells	Synapses	Synapses /J7 cell	J7 cells with 1 synapse, %	J7 cells with 2 synapses, %	J7 cells with 3 synapses, %
Experiment 1							
Ly49A	66.8 ± 10.7	59.0 ± 12.8	53.0 ± 7.2	0.92 ± 0.11	38.64	21.02	2.03
ANKD-CST	57.0 ± 6.3	46.8 ± 9.2	39.6 ± 8.9	0.84 ± 0.08	38.03	17.52	2.14
ANKD-HST	62.4 ± 14.7	54.6 ± 10.5	29.8 ± 12.2	0.54 ± 0.18	26.70	10.62	1.10
Ly49A-ST2	53.4 ± 4.5	50.8 ± 2.2	0.0	0.00	0.00	0.00	0.00
Experiment 2							
Ly49A	64.6 ± 4.5	55.2 ± 6.4	53.6 ± 8.8	0.98 ± 0.15	29.71	21.38	6.88
ANKD-CST	66.8 ± 11.8	53.0 ± 7.2	45.2 ± 6.1	0.86 ± 0.12	34.34	15.47	5.28
ANKD-HST	60.2 ± 10.1	57.6 ± 4.6	29.0 ± 8.4	0.51 ± 0.18	22.57	10.42	2.08
Ly49A-ST2	57.4 ± 10.6	41.2 ± 6.1	0.0	0.00	0.00	0.00	0.00
Experiment 3							
Ly49A	73.8 ± 8.5	58.2 ± 5.9	49.8 ± 4.9	0.86 ± 0.08	42.96	17.18	2.41
ANKD-CST	67.8 ± 9.7	61.4 ± 8.2	46.8 ± 4.8	0.77 ± 0.08	41.04	11.07	2.93
ANKD-HST	58.0 ± 8.2	52.0 ± 11.8	31.0 ± 7.3	0.60 ± 0.08	33.08	9.62	1.92
Ly49A-ST2	67.4 ± 4.9	54.6 ± 7.2	0.0	0.00	0.00	0.00	0.00

In each experiment, 5 independent images were collected for each receptor. Cell numbers and synapses were counted in each image, and the average numbers from 5 images are presented. Data for Synapse/J7 were combined from 3 experiments, and multiple comparisons were performed using Sidak *t* test. *P* of all the comparisons, except for the combination of Ly49A and ANKD-CST, was <0.001; therefore, they were statistically different (*P* for Ly49A and ANKD-CST was 0.027; therefore, it was not significant in multiple comparisons).

Other Supporting Information Files

Appendix